Modulating Cell Behaviors on Chiral Polymer Brush Films with Different Hydrophobic Side Groups

Xing Wang,[†,§,⊥] Hui Gan,[†,∥,⊥] Mingxi Zhang,[‡] and Taolei Sun*,[†,‡]

[†]Physikalisches Institut, WWU Muenster, Muenster 48149, Germany

[‡]State Key Lab of Advanced Technology for Materials Synthesis and Processing, Wuhan University of Technology, Wuhan 430070, China

[§]College of Life Science and Technology, Beijing University of Chemical Technology, Beijing 100029, China

[∥]Institute of Transfusion Medicine, Academy of Military Medical Sciences, Beijing 100850, China

Ⓢ Supporting Information

ABSTRACT: Chirality is one of the significant biochemical signatures of life. Nearly all biological polymers are homochiral as they usually show high preference toward one specific enantiomer. This phenomenon inspires us to design biomaterials with chiral units and study their interactions with cells and other biological entities. In this article, through adopting three pairs of aliphatic amino acids with different hydrophobic side groups as chiral species, and using two adhesive cell lines as examples, we show that the chirality of polymer brushes can trigger differential cell behaviors on the enantiomorphous surfaces, and more interestingly, such chiral effect on cellular behaviors can be modulated in a certain extent by varying the hydrophobic side groups of the chiral moieties composing the polymers. This work not only proves the versatility of the chiral effect at the cell level but also demonstrates a method to bridge the gap between organic signal molecules and biomaterials. It thus points out a promising approach for designing novel biomaterials based on the chiral effect, which will be an important complement for conventional strategies in the study of biomaterials.
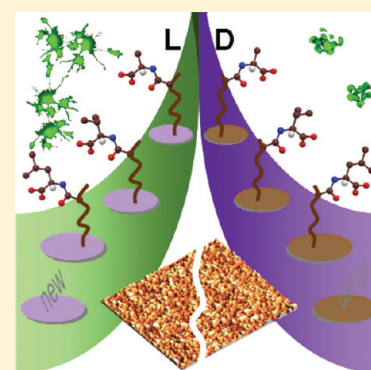
1. INTRODUCTION

The boom of modern biomaterials from lab to hospital is a part of achievements on deeper understanding how biomaterials interact with the biological systems at both the cellular and molecular level, with the ultimate purpose to create more suitable materials and products.[1−6] Study of the interaction between cells and artificial materials is a fundamental focus in the biomaterials research frontier. Attention to the molecular and structural information coded within the biointerface, acting as the extracellular milieu, is intensively inspiriting the development of novel biomaterials. Although several important extracellular factors, including functional groups, charges, wettability, roughness, and geometry, etc., have been studied to regulate cell fate,[7−9] further exploring cell behaviors on material surface is highly desirable as we are still at the primary stages of learning how to design and control the material properties to gratify the need of medical treatment. Recently, we found that chirality is another promising factor in biomaterial design, especially for the treatment of surface or interface, which can influence biological processes such as protein adsorption, cell adhesion, and consecutive behaviors.[10−12] However, it is necessary to understand how the chemical structures of chiral moieties influence cell behaviors on the surface of materials, since it directly governs the applications of chiral effect in practical systems.

Chiral polymer brush films provide an ideal platform to study this topic.[13,14] On the one hand, polymers are the mostly common-used biomaterials,[14−17] and many copolymers have been used successfully to produce multiple styles of functional surfaces for various bioassays.[18,19] On the other hand, polymer brushes show obvious advantages of easy tailorability over their chemical compositions, properties, and functions, which brings great convenience to introduce chiral functional units into the polymer chains via copolymerization or terminal group modification. Furthermore, nearly all biological polymers (proteins, RNA, DNA, etc.) are homochiral.[20,21] Amino acids, as one of the fundamental materials in life whose chirality determines the steric configurations and higher-order conformations of proteins and other biomacromolecules,[22] are preferential candidates for biopolymer design or simulation, and their chiral natures as modulating factors are instinct. In addition, acryloyl polymer is recognized as a promising candidate for biocompatible materials,[17] which is easy to bear functional groups as side chains. Therefore, here we developed a model system of chiral polymer brushes with an achiral polyacryloyl backbone bearing amino acids on side chains as chiral comb-teeth, as shown in Scheme 1.

Scheme 1. Schematic Representation for the Preparation of the Chiral Polymer Brush Films[a]
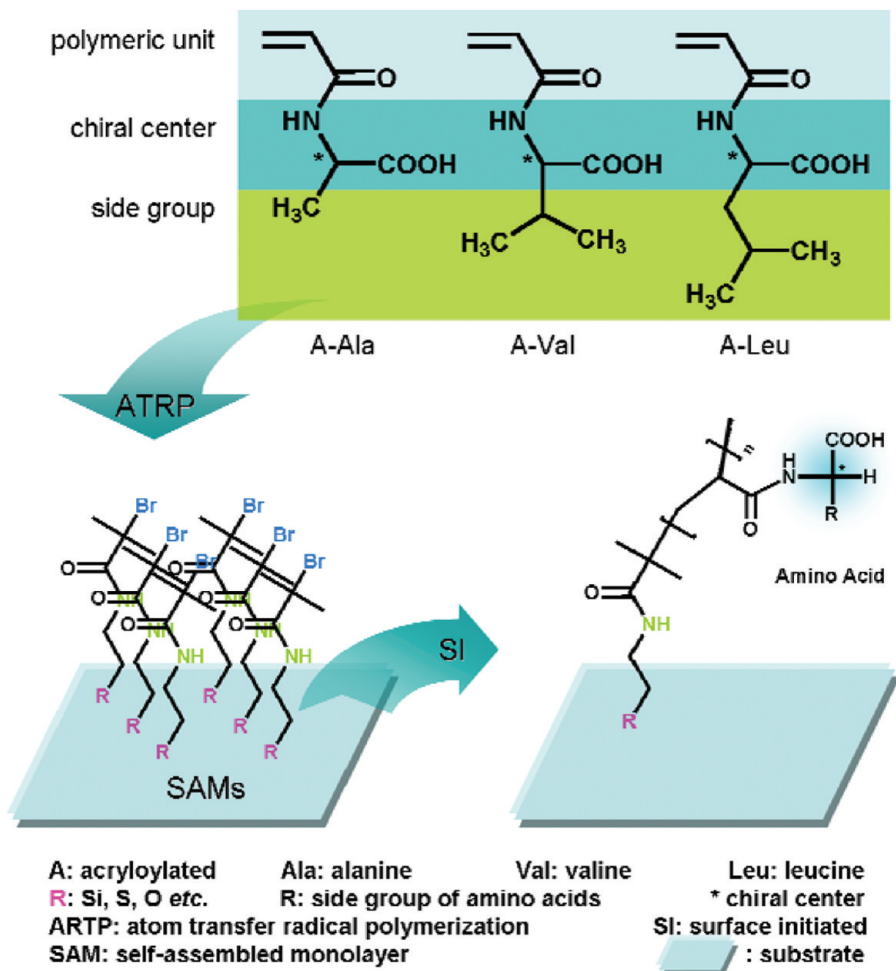
[a]For this strategy, the comblike polymer, bearing chiral amino acid comb-teeth as a kind of modulator, can be tethered on various substrates (silicon was used here). Three pairs of amino acids, including L(D)-alanine, L(D)-valine, and L(D)-leucine, were employed in this article; the final tethered polymer brushes were denoted as L(D)-PA, L(D)-PV, and L(D)-PL, respectively.

In this study, through adopting three pairs of chiral polymer brush films based on aliphatic amino acids with different sizes of hydrophobic side groups (Scheme 1) and studying the behaviors of two kinds of adhesive cell lines, we address here that the side-group size has great influence on the stereo-selective interaction between cells and chiral polymer surfaces, in which a larger side group leads to a more distinct difference on cellular behaviors between the L(D) surfaces, whereas for the polymer with a small side group (e.g., $-CH_3$ group), the chiral effect is insignificant. This demonstrates an effective strategy to design chiral polymer brush films that enables us to use stereochemistry to regulate cell behaviors.

2. EXPERIMENTAL SECTION

The polymer brushes were fabricated on silicon (Si) substrates using the proven method of surface initiated atom transfer radical polymerization (SI-ATRP, see Scheme 1).[23] A clean Si substrate was first treated to generate surface hydroxy groups. After dried under a nitrogen flow, it was immersed and heated to reflux in toluene with 5 wt % ATMS for 3 h to obtain surface $-NH_2$ groups. Then it was rinsed with toluene and dichloromethane, dried, and immersed in dichloromethane with 2 vol % pyridine. Appropriate amount of bromoisobutyryl bromide was added dropwise into above solution at 0 °C, and the mixture was left for 1 h at this temperature and then at room temperature for 12 h. The substrate was cleaned with dichloromethane and toluene. Polymerization was achieved by immersing the dried substrate in a degassed solution of N-acryloyl-L(D)-amino acid monomer (4 mmol) in a 1:1 (v/v) mixture of H_2O and MeOH (8 mL) containing Cu(I)Br (23 mg) and PMDETA (0.1 mL) for 3 h at 60 °C. After grafting polymer brush on Si surface, it was immersed in and rinsed with methanol, ethanol, and deionized water, respectively, to remove all the possible impurities. Under these conditions, the film thickness was about 12 ± 2 nm. As three pairs of amino acids including L(D)-alanine, L(D)-valine, and L(D)-leucine were employed here, the final grafted polymer brushes were denoted as L(D)-PA, L(D)-PV, and L(D)-PL, respectively. For additional details, see the Supporting Information.

African green monkey SV-40 transformed kidney fibroblast cell line (COS-7) and mouse brain endothelial cell line (bEnd.3) were cultured in Dulbeccos Modified Eagles Medium (DMEM) (GIBCO, Germany) until they reached appropriate coverage of plates and showed typical cell morphology. Cells were digested with 0.25% trypsin−EDTA solution (Sigma) in PBS (pH 7.4) and seeded on the chiral polymer brush films at 5×10^4 COS-7 cells per well and 1×10^5 bEnd.3 cells per well in 24-well plates (Corning, Germany) for cell culture experiments. The cultures were incubated at 37 °C, and the observations were made at 10 min, 1 h, 24 h, and 48 h time points. The medium was changed every 2 days. All experiments were performed at least six times. For additional details, please see the Supporting Information.

CellTracker Green CMFDA (Invitrogen, Germany) was used for long-term tracing of living cells, and cell morphology was observed and imaged by fluorescence microscope (Axioskop 2 plus, Zeiss, Germany). At least 1/5 areas were taken micrographs from random areas of each surface. Cell numbers of images were processed with ImageJ software. Each cell was fit to the shape of an ellipse using the "analyze particle" command, and the number of cells within each image was counted. Photoshop CS and Volocity (Improvision) software were used for image processing of the cell surface area (2D) and total fluorescent intensity (3D). Statistical analysis was performed on the SigmaPlot 11.0 statistical package, and values were considered significant at $P < 0.05$. The student's t test was used to compare the data for the sample and control groups.

3. RESULTS AND DISCUSSION

3.1. Characterizations on Polymer Brush Films.
Our recent studies indicated that the SI-ATRP method is harmless for the chirality in this polymeric system.[12] As shown in Figure S1, the UV−vis and circular dichroism (CD) measurements show that the optical rotation has been largely amplified after the polymerization process compared with the original monomer. The reason is that the chiral units assemble in a regular way, which largely constrains the freedom of the chiral units and thus greatly enhances the overall chirality of the system, especially on the two-dimensional tethered polymer brushes. Therefore, under the same reaction conditions, the polymer films exhibit opposite chirality, but their other physical and chemical properties of the polymer brush films based on the enantiomers of the same amino acid are identical.

The atom force microscope (AFM) measurement was first used to detect the surface topography of these films. As shown in Figure 1 for the three-dimensional profiles, they are similar in
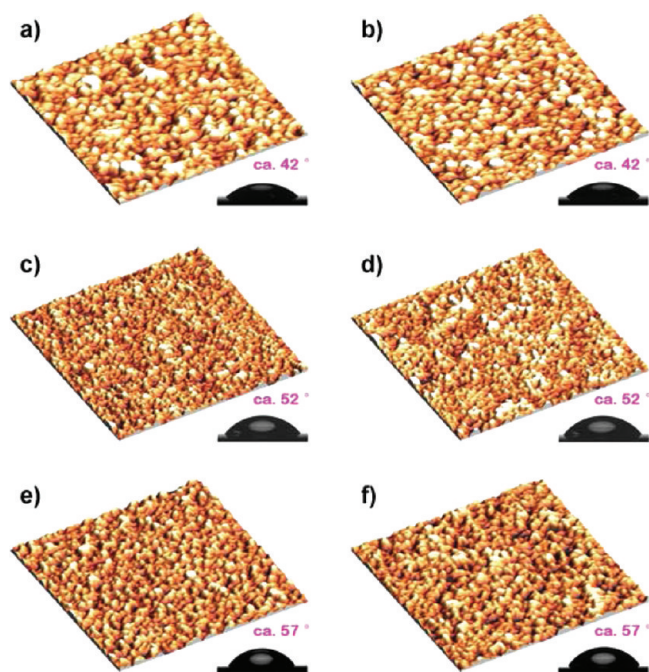

Figure 1. Topography of the films: (a) L-PA; (b) D-PA; (c) L-PV; (d) D-PV; (e) L-PL; (f) D-PL identified by AFM (1×1 μm; $Z = 5$ nm) and the corresponding wettability studies. The water CA measurements show that the films are hydrophilic with CAs of about 42° for PA, about 52° for PV, and about 57° for PL, but there is no difference between a pair of enantiomerphous surfaces.

surface morphology and quite uniform with the roughness below 2 nm; the nanoscaled random coils come into being on the substrate (see the height images in Figure S2), and the polymer brushes cover the whole surface uniformly (see the phase images in Figure S2). Even in a large scale up to hundreds of micrometers, the films also exhibit relatively smooth feature, as indicated by the ellipsometry studies (see Figure S3). These analyses show the advantages of tethered polymer brush summarized as follows: (i) high coverage and no overlapping for polymer brush chains on the surface,[14] (ii) high density of functional groups on the surface,[15] (iii) easy formation of nanoscale topography on the polymer film, and (iv) high stability of covalent linkage to the surface.[11−17,23−25]

However, the wettability of the films is very different due to the molecular structures of the hydrophobic side groups of amino acids. As shown in the insets of Figure 1, the static contact angles (CAs) increase regularly with the increase of sizes of the hydrophobic side groups from methyl to isopropyl, further to isobutyl, which vary from about $42 \pm 1°$ for the L(D)-PA films to about $52 \pm 2°$ for the L(D)-PV films, and further to about $57 \pm 2°$ for the L(D)-PL films. For all these films, a pair of enantiomorphous surfaces is identical in wettability, indicating that surface chirality does not influence the surface free energy of the films.

3.2. Behaviors of COS-7 Cells on Chiral Polymer Brush Films.
As one of the main cellular components for human tissues, fibroblasts are widely used to evaluate the cellular response of artificial biomaterials.[26,27] Here, typical fibroblast cell line COS-7 cells (derived from kidney cells of the African green monkey) were employed first to investigate the cell behaviors on all the chiral polymer brush films, considering that COS-7 has a symbolic branched cytoplasm and individual COS-7 cells can also migrate slowly over substrate, which would provide plentiful knowledge about the cell/substrate interactions. As we pay more attention to studying the cell/surface interactions, the fluorescent microscopy is preferred because of its intuitional manner, which focuses on the surface for studying cell behaviors *in situ*. Each experiment was performed for at least six times, in which classical fluorescent microscopy and statistical calculations were adopted to explore cell behaviors during different periods of cell incubation.

In the initial 10 min of incubation, a small amount of COS-7 cells was found to attach onto the films, and all cells were distributed separately with round morphology (see Figure S4a). There was nearly no difference in this period for cell touching on all the six surfaces. However, along with the extending of incubation, more and more cells adhered onto the surfaces, where clear differences could be observed after 1 h of incubation (see Figure 2a/d,g/j,m/p). The cell numbers on all the L-films were apparently higher than those on the corresponding D-films. The data of cellular density, as listed in Table 1, show that the numbers of cells on the L-films almost doubled those on the corresponding D-films for all three kinds of polymers. These phenomena give a clear hint that cells prefer the L-surface to the D-surface. However, the results of t test (P value) revealed that the densities of cell adhesion between the L(D)-surfaces had statistical difference on both the PV and PL films ($P < 0.05$), whereas it was not significant on the PA films ($P > 0.05$), though the average value on the L-PA surface was higher than that on the D-PA surface. We speculate that the smaller methyl group of L(D)-alanine supplied relatively weaker chiral characterization instead of lower hydrophobicity because the cell densities on the L(D)-PA films were close to
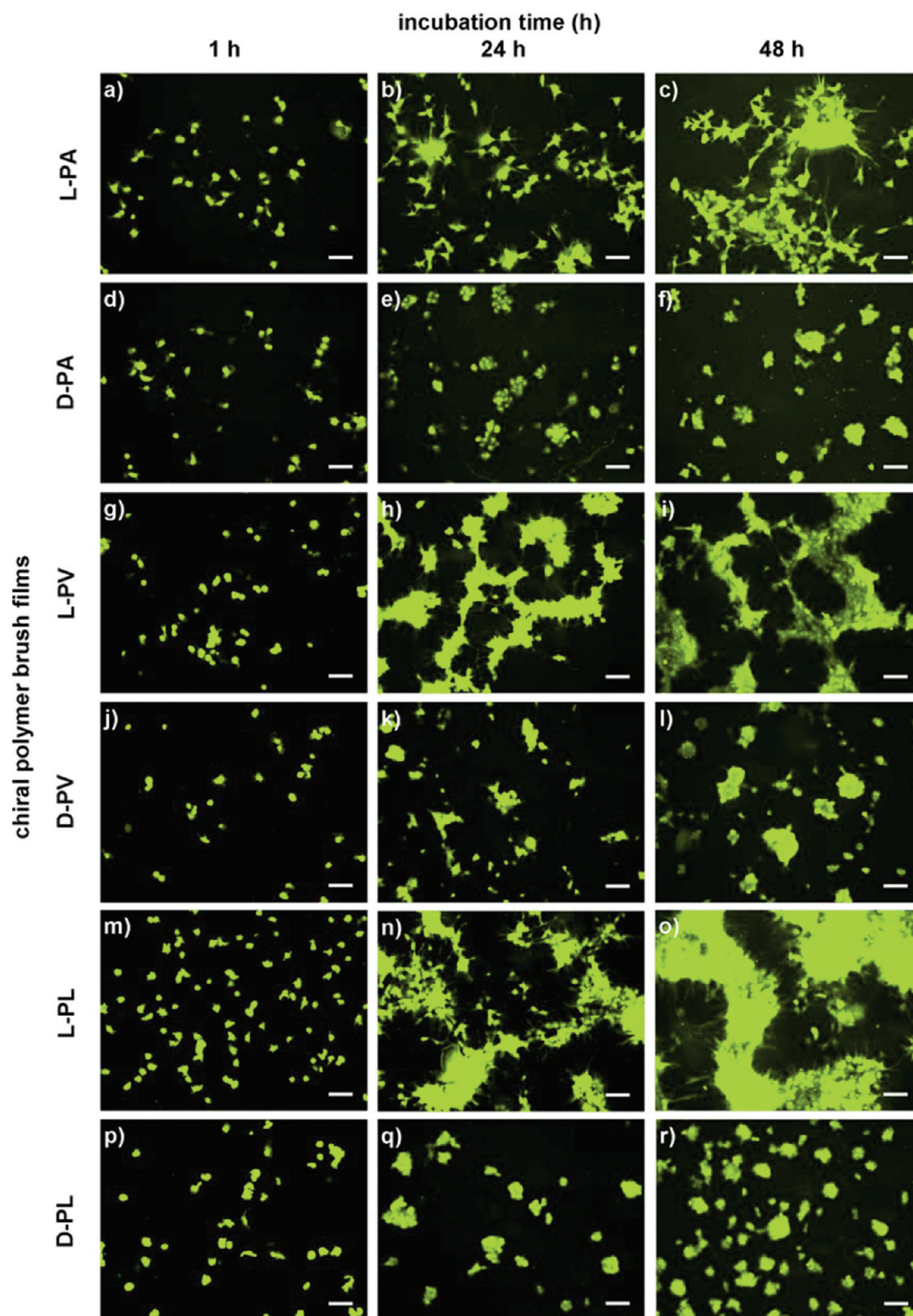
Figure 2. Typical fluorescent images of COS-7 cells incubated at different time periods on the chiral polymer brush films. Scale bars: 100 μm.

those on the L(D)-PV films. Nevertheless, the L(D)-PL films exhibited higher ability for cell adhesion since higher cell densities were observed (Table 1), indicating that larger alkyl side group and the subsequent higher hydrophobicity of the surface are favorable for cell adhesion. In our opinion for this period, chirality of the branch terminal induced a larger difference for cell adhesion between the L(D)-films compared with other factors such as the change of side groups and surface wettability for the three kinds of polymer films used here.

Table 1. Cell Densities for 1 h Incubation of COS-7 Cells on the Chiral Polymer Brush Films

polymer brush	cell density ($\times 10^3$ cm^{-2})		t test[a]
	L-film	D-film	P value
PA	4.78 ± 1.78	2.93 ± 0.68	0.100
PV	4.17 ± 1.52	2.50 ± 1.06	0.007
PL	6.72 ± 2.23	3.72 ± 1.22	0.030

[a]The statistic analysis is based on 6 times of cell culture experiments.

By prolonging the incubation time from 1 to 24 h (see Figure 2b/e,h/k,n/q), new aspects with significant differences were observed. Besides that the cell densities increased on all six surfaces, a more interesting aspect was that the cell morphology and configuration exhibited great differences between the L(D)-films. Cells on the L-films (Figure 2b,h,n) seemed to have higher activity: they spread on the surface and connected to each other to form large interlinked clusters, where more pseudopodia were presented. Otherwise on the D-films (Figure 2e,k,q), cells preferred to remain isolated stacks with a roughly round morphology. When the incubation time was prolonged to 48 h (see Figure 2c/f,i/l,o/r), the above differences became more significant. The growth, spreading, and connection of cells shaped them into large and highly interconnected two-dimensional assemblies on the L-films (Figure 2c,i,o). However, on the D-films (Figure 2f,l,r), it shows that cells could not form effective connections with each other through the guidance of the substrates. Instead, cells more preferred to grow on the top of other cells and formed the isolated clusters. Since cells respond to the surfaces instinctually, it could be concluded that the stereochemistry greatly influence the cell growth and spreading behaviors on the polymer brush films. It might be further deduced that the chiral modulation runs on the opposite directions: being improved by the L-enantiomers, whereas being suppressed by the D-enantiomers.

Another feature could be noticed that the sizes of the hydrophobic side groups also have regular influence on cellular behaviors on the polymer brush films. After the same incubation time, especially for the L-films as shown in Figure 2, the extent of cell spreading and connection increased with the groups' sequence of alanine, valine, and leucine, indicating that increasing the size of hydrophobic side groups of the L-polymers could significantly improve the cell activity on surface. However, on the D-films, the difference among the three surfaces was much smaller, where the piling-up cell stacks almost kept round morphologies and few pseudopodia were extruded. There was no evidential expansion of cell density on them compared with that on the L-films, though the changing of wettability is same following the sequence of the PA, PV, and PL films. Thus, these results suggest that the L-enantiomers of the amino acid units could effectively influence cell behaviors within a wide range compared with the D-enantiomers. On the other hand, along with the elongation of the incubation time (see Figure 2), the cell proliferation seemed to process at different speeds, and their differentiation and migration on the surfaces were also different, resulting in diverse gradable cell densities on the PA, PV, and PL films. This indicates that many kinds of cellular behaviors could also be modulated by changing the chiral moieties in this polymer brush system.

For long-time incubation (24 and 48 h), the cell−cell contact and the cells assembly performed more prominent features. Therefore, the analysis of cell density became difficult owing to the complicated cell overlapping. To address this issue, we used

another two parameters to evaluate cell behaviors. The quantitative characterizations were performed through analyzing the fluorescent images by Photoshop CS (Adobe) and Velocity (Improvision) software.[28,29] The former provides the area ratio (A_r) for the cell-covered section, describing the two-dimensional cell spreading on the surface; the latter calculates the integral fluorescent intensity (I_f) for the cell-occupied regions, which gave a three-dimensional expression for the volume of cells on the substrate.

As shown in Figure 3 (see Supporting Information for the data details), the average A_r values (Figure 3a) on the L-films
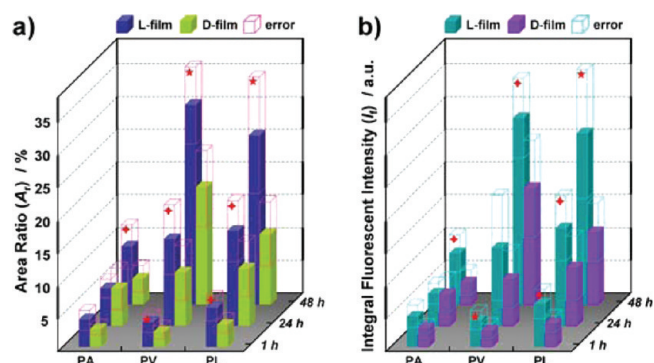

Figure 3. Analytical results of COS-7 cells adhered on the chiral polymer brush films based on the fluorescent images. (a) The area ratio method. (b) The integral fluorescent intensity method. The t test: $P < 0.05$ (◆); $P < 0.01$ (★).

were much higher than those on the corresponding D-films at all analyzed time points on the three kinds of polymer brush films. Statistical significance was shown finally on the PA films after 48 h (t test: $P < 0.05$). The increasing tendencies both followed the time axes distinctly and were along with the increase of size of the hydrophobic side groups. This graph was consistent with above results; the data demonstrated not only the differential growth and assembly of COS-7 cells on these chiral surfaces but also the changing regulation mediated by the molecular structures of chiral moieties from methyl to isopropyl, further to isobutyl. Simultaneously, the three-dimensional calculations simulated by I_f value (Figure 3b) well supported aforesaid conclusions (discussion in Figure 2) for the cell proliferation, differentiation, and migration.

As a brief summary, such differential cell behaviors reveal that the L-polymer brush films have much higher cytocompatibility than the D-films. Importantly, the function of the chiral film can be modulated to a certain extent by changing the molecular structures of chiral moieties. As a result, the larger size of hydrophobic side group induces much significant difference on cellular behaviors. It presents a clear strategy to design novel chiral materials or surfaces to regulate cell behaviors.

3.3. Behaviors of bEnd.3 Cells on Chiral Polymer Brush Films. As a new type of biomaterial potentially for biomedicine or tissue engineering, more understanding on cytocompatibility is inevitable due to the complexity of biosystems. A different cell line bEnd.3 (derived from mouse brain endothelial cells) was thus selected as another object in our research. Different from fibroblasts that mainly exist in connective tissues, bEnd.3 cells are endothelial cells, which lie in the entire circulatory system throughout the body, and act as

selective barriers between the vessel lumen and the surrounding tissues.[30,31]

In the earliest 10 min, bEnd.3 cells displayed the round morphology (see Figure S4b) and no difference was found, as well as COS-7 cells, on all the six surfaces. After 1 h incubation of bEnd.3 (see Figure 4a/d,g/j,m/p), besides the increased cell
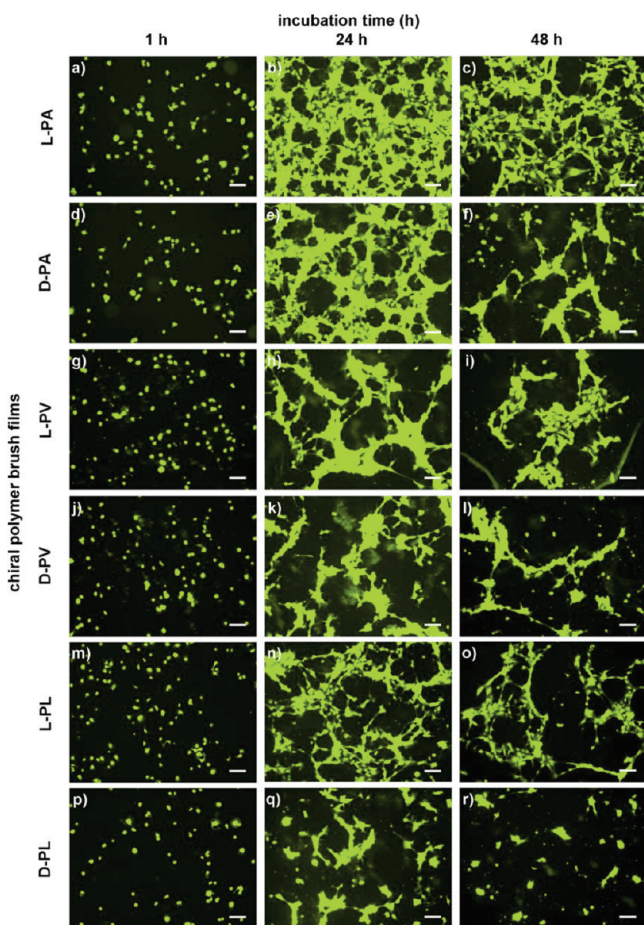

Figure 5. Analytical results of bEnd.3 cells adhered on the chiral polymer brush films based on the fluorescent images. (a) The area ratio method. (b) The integral fluorescent intensity method. The *t* test: $P < 0.05$ (◆); $P < 0.01$ (★).

Figure 4. Typical fluorescent images of bEnd.3 cells incubated at different time periods on the chiral polymer brush films. Scale bars: 100 μm.

quantities, nearly all cells were still round morphology. It is noteworthy that except for the case of PL films (Table 2),

Table 2. Cell Densities for 1 h Incubation of bEnd.3 Cells on the Chiral Polymer Brush Films

| polymer brush | cell density ($\times 10^3$ cm^{-2}) | | *t* test[a] |
	L-film	D-film	*P* value
PA	8.31 ± 3.62	5.78 ± 2.94	0.320
PV	6.90 ± 2.08	6.77 ± 2.26	0.914
PL	10.68 ± 1.74	6.12 ± 0.30	0.011

[a]The statistic analysis is based on 6 times of cell culture experiments.

where the cell density was significantly larger on the L-surface than that on the D surface ($P < 0.05$), no statistical difference ($P \gg 0.05$) were found on both PA and PV films.

However, after 24 h incubation (see Figure 4b/e,h/k,n/q), the cells multiplied and contacted with each other, resulting in dense networks on all films, and an important result was presented that the statistical difference between the L(D)-PV films became distinct (Figure 5a, see Supporting Information
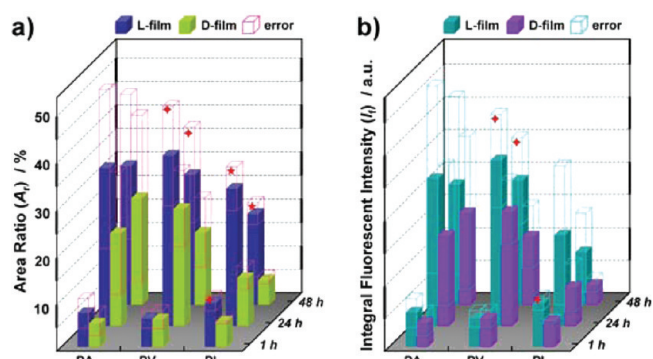
for the data details), where the L-PV film had higher average A_r values than the corresponding D-PV film ($P < 0.05$), whereas the statistical significance did not change for the PA and PL films (the *P* value is still more than 0.05 for PA films and still less than 0.05 for PL films). This phenomenon implied the modulating function of the molecular structure of chiral moiety, since the larger isobutyl triggered differential cell behaviors on the enantiomerphous surfaces earlier and more effectual than the middling isopropyl, further than the smaller methyl. This is similar to the results of COS-7 cells as mentioned above. However, after 48 h incubation (see Figure 4c/f,i/l,o/r), the statistical difference did not show on the PA films (Figure 5), expectantly. But, a new phenomenon came into being at this time point; the cell numbers decreased with obvious reduction compared with the results of 24 h on all kinds of films. The reductions were caused by the apoptotic or necrotic cell death since dead cells normally would leave the surface.[32−34] Though cell death happened, the calculated results (Figure 5) also pointed out a clear difference between the L(D)-surfaces on both PV and PL films. In addition, it might be worthy of note that the *t* test of I_f values (Figure 5b) on the PL films showed changes on the statistical significance compared with the A_r analysis (Figure 5a) after 24 h. The netlike growth property of reticuloendothelial bEnd.3 cells was considered to be the reason. Nevertheless, the L-polymer brushes have much higher cytocompatibility than the corresponding D-films, and the modulating function of chiral groups is positive.

Interestingly, along with the film sequence of PA, PV to PL, bEnd.3 cells seem to show an opposite trend on the polymer brushes compared with COS-7 cells. On one hand, it seems that the PA films are more preferable for bEnd.3 cell in culture than the PV films, further better than the PL films (Figure 4). However on the other hand, the PA films did not show the statistical difference between the L(D)-films even after 48 h, whereas the PL films triggered differential cell behaviors at very early stage of 1 h (Figure 5); these phenomena suggest that maybe surface wettability is a major influences on governing the biological tissue specificity (bEnd.3 prefers hydrophilic surface other than COS-7), whereas chiral signature or component coded in polymer film may dominate the cells responding. It further demonstrates the advantage of this chiral biomimetic strategy for biological applications.

It is obvious that different cells sense the chiral polymer brush films in their own manner. The possible reasons behind the above-mentioned cell behaviors could be attributed to the

Scheme 2. Schematic Representation of Cell-Surface Interaction Proposed for Cellular Sensing and Responding on the Chiral Polymer Brush Films[a]
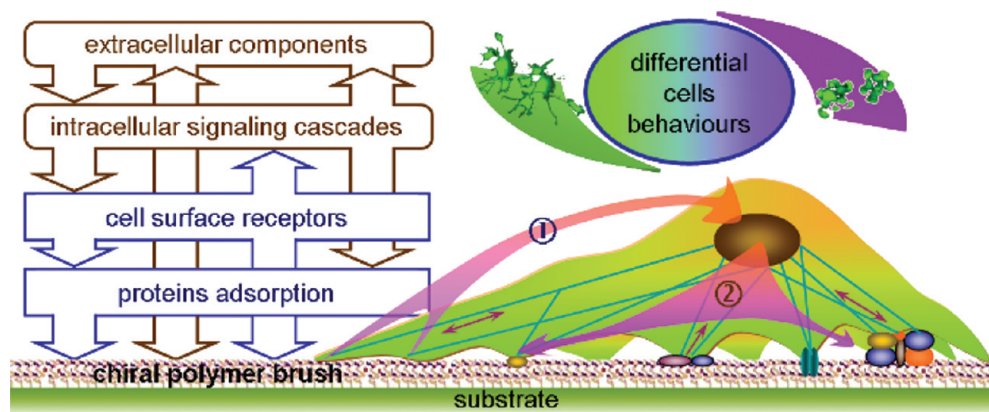
[a]Differential cell behaviors exhibit on the enantiomorphous surfaces, and the chiral moieties of the comblike polymer brush act as a controllable factor on modulating above differential cell behaviors to a certain extent.

differential stereoselective recognition and binding between the surface chiral moieties of the polymer brush films and the cells. As live-cell's surface is much more complex than polymer substrate, study of cell-surface interaction should follow the cellular sense and the characters donated by the polymer brushes. As shown in Scheme 2 for a schematic study, cell surface receptors respond to the chiral surfaces directly[35,36] or are induced by surface proteins indirectly, since protein adsorption is generally the first event that happens during the material contacts with biological environments and potentially leads to the exposure of specific epitopes for cell adhesion.[18,37,38] The surface proteins usually have a strong influence on the following biological events. Recently, we have found that protein adsorption also displayed differential actions on this kind of enantiomorphous surfaces.[11] The corresponding thermodynamic analysis demonstrated that the stereoselective hydrophobic interaction is the main driving force for this effect, which is maybe related to the conformational matching or not between the terminal chiral moieties of the polymers and the hydrophobic domains of proteins. Therefore, both the adsorption and the revealed conformation of surface proteins might play the key role for the subsequent cells response. Although it might be an indirect signaling process during cell adhesion, it is still possible to use chiral surfaces to modulate cell behaviors because both the complex intracellular signaling cascades and the bidirectional interactions on extracellular components are associated with chiral surface in/directly[39−41] and then followed with differential cell behaviors and functions. Study on this topic may bring more inspirations, not only on further understanding of cell-surface interactions but also on the design of next generation of biointerface based on the chiral effect.

4. CONCLUSION

From a point of view of biomaterials, (I) the stereochemistry design on the polymer brushes can trigger differential cell behaviors on the enantiomerphous surfaces, (II) changing the molecular structures of the chiral moieties within the biomaterials can be used to regulate multifold cell behaviors on the surface in a certain extent, (III) generally, the L-films have higher cytocompatibility, and (IV) the design and application of chiral biomaterials strongly depend on the specific biological tissues and cells. From a point of view of

biology, cells can distinguish the extracellular milieu on molecular level of the steric configurations and then response to them in a chiral-dependent manner. Therefore, this study helps us to know that what kind of chiral factors are good for cellular behaviors. Compared to our previous studies of immune cell behaviors on the chiral self-assembly surfaces, the chiral polymer brush strategy not only proved the versatility of the chiral effect but also bridged the gap between small organic functional molecules and chiral biopolymer materials. We believe that the chiral effect reported here will act as an important complement for conventional strategies in the study of biomaterials.

■ ASSOCIATED CONTENT

⑤ Supporting Information
Experimental details, spectral characterizations for the polymerization of the chiral polymers, AFM and ellipsometry images of the polymer brushes, and analytical data of cells culture experiments. This material is available free of charge via the Internet at http://pubs.acs.org.

■ AUTHOR INFORMATION

Corresponding Author
*E-mail: suntaolei@iccas.ac.cn.
Author Contributions
⊥These authors contributed equally to this work.

■ ACKNOWLEDGMENTS

■ REFERENCES

(1) Langer, R.; Tirrell, D. A. *Nature* **2004**, *428*, 487−492.
(2) Langer, R.; Vacanti, J. P. *Science* **1993**, *260*, 920−926.
(3) Somorjai, G. A.; Frei, H.; Park, J. Y. *J. Am. Chem. Soc.* **2009**, *131*, 16589−16605.
(4) Place, E. S.; Evans, N. D.; Stevens, M. M. *Nature Mater.* **2009**, *8*, 457−470.
(5) Nel, A. E.; Mädler, L.; Velegol, D.; Xia, T.; Hoek., E. M. V.; Somasundaran, P.; et al. *Nature Mater.* **2009**, *8*, 543−557.
(6) Peppas, N. A.; Langer, R. *Science* **1994**, *263*, 1715−1720.

(7) Mei, Y.; Saha, K.; Bogatyrev, S. R.; Yang, J.; Hook, A. L.; Kalcioglu, Z. I.; et al. *Nature Mater.* **2010**, *9*, 768−778.

(8) Mitragotri.; Lahann, J. *Nature Mater.* **2009**, *8*, 15−23.

(9) Lim, J. Y.; Hansen, J. C.; Siedlecki, C. A.; Hengstebeck, R. W.; Cheng, J.; Winograd, N.; et al. *Biomacromolecules* **2005**, *6*, 3319−3327.

(10) Sun, T.; Han, D.; Riehemann, K.; Chi, L.; Fuchs, H. *J. Am. Chem. Soc.* **2007**, *129*, 1496−1497.

(11) Wang, X.; Gan, H.; Sun, T. *Adv. Funct. Mater.* **2011**, *21*, 3276−3281.

(12) Wang, X.; Gan, H.; Sun, T.; Su, B.; Fuchs, H.; Vestweber, D.; et al. *Soft Matter* **2010**, *6*, 3851−3855.

(13) Ratner, B. D.; Bryant, S. J. *Annu. Rev. Biomed. Eng.* **2004**, *6*, 41−75.

(14) Senaratne, W.; Andruzzi, L.; Ober, C. K. *Biomacromolecules* **2005**, *6*, 2427−2448.

(15) Tugulu, S.; Silacci, P.; Stergiopulos, N.; Klok, H. A. *Biomaterials* **2007**, *28*, 2536−2546.

(16) Mizutani, A.; Kikuchi, A.; Yamato, M.; Kanazawa, H.; Okano, T. *Biomaterials* **2008**, *29*, 2073−2081.

(17) Brun-Graeppi, A. K. A. S.; Richard, C.; Bessodes, M.; Scherman, D.; Merten, O.-W. *Prog. Polym. Sci.* **2010**, *35*, 1311−1324.

(18) Chen, H.; Yuan, L.; Song, W.; Wu, Z.; Li, D. *Prog. Polym. Sci.* **2008**, *33*, 1059−1087.

(19) Wischerhoff, E.; Uhlig, K.; Lankenau, A.; Boerner, H. G.; Laschewsky, A.; Duschl, C.; et al. *Angew. Chem., Int. Ed.* **2008**, *47*, 5666−5668.

(20) von der Mark, K.; Park, J.; Bauer, S.; Schmuki, P. *Cell Tissue Res.* **2010**, *339*, 131−153.

(21) Haupt, K. *Nature Mater.* **2010**, *9*, 612−614.

(22) Chela-Flores, J. *Chirality* **1994**, *6*, 165−168.

(23) Sun, T.; Wang, G.; Feng, L.; Liu, B.; Ma, Y.; Jiang, L.; et al. *Angew. Chem., Int. Ed.* **2004**, *43*, 357−360.

(24) Qing, G.; Wang, X.; Jiang, L.; Fuchs, H.; Sun, T. *Soft Matter* **2009**, *5*, 2759−2765.

(25) Wang, X.; Qing, G.; Jiang, L.; Fuchs, H.; Sun, T. *Chem. Commun.* **2009**, 2658−2660.

(26) O'Connell, D. J.; Molinar, A. J.; Tavares, A. L.; Mathine, D. L.; Runyan, R. B.; Bahl, J. J. *Life Sci.* **2007**, *80*, 1395−1402.

(27) Ma, D.; Chen, H.; Li, Z.; He, Q. *Biomicrofluidics* **2010**, *4*, 044107.

(28) Hand, A. J.; Sun, T.; Barber, D. C.; Hose, D. R.; Macneil, S. *J. Microsc.* **2009**, *234*, 62−79.

(29) Benedito, R.; Roca, C.; Sörensen, I.; Adams, S.; Gossler, A.; Fruttiger, M.; et al. *Cell* **2009**, *137*, 1124−1135.

(30) Zhang, H.; Mitin, A.; Vinogradov, S. V. *Bioconjugate Chem.* **2009**, *20*, 120−128.

(31) Douville, N. J.; Tung, Y.-C.; Li, R.; Wang, J. D.; El-Sayed, M. E. H.; Takayama, S. *Anal. Chem.* **2010**, *82*, 2505−2511.

(32) Acharya, A. P.; Dolgova, N. V.; Clare-Salzler, M. J.; Koselowsky, B. G. *Biomaterials* **2008**, *29*, 4736−4750.

(33) Chen, C. S.; Mrksich, M.; Huang, S.; Whitesides, G. M.; Ingber, D. E. *Science* **1997**, *276*, 1425−1428.

(34) Webb, K.; Hlady, V.; Tresco, P. A. *J. Biomed. Mater. Res.* **2000**, *49*, 362−368.

(35) Hynes, R. O. *Cell* **1992**, *69*, 11−25.

(36) Hazen, R. M.; Sholl, D. S. *Nature Mater.* **2003**, *2*, 367−374.

(37) Roach, P.; Farrar, D.; Perry, C. C. *J. Am. Chem. Soc.* **2005**, *127*, 8168−8173.

(38) Horbett, T. A., Brash, J. L., Eds.; *ACS Symposium Series 602*; American Chemical Society: Washington, DC, 1995; pp 1−23.

(39) Vogel, V.; Sheetz, M. *Nat. Rev. Mol. Cell Biol.* **2006**, *7*, 265−275.

(40) Gan, H.; Tang, K.; Sun, T.; Hirtz, M.; Li, Y.; Chi, L.; et al. *Angew. Chem., Int. Ed.* **2009**, *48*, 5282−5286.

(41) Tang, K.; Gan, H.; Li, Y.; Chi, L.; Sun, T.; Fuchs, H. *J. Am. Chem. Soc.* **2008**, *130*, 11284−11285.